In-plane polarization transfer in the ^{6}Li(p,p') reaction and the effective NN interaction

Y. Nakai, M. Nakamura, H. Sakaguchi, H. Togawa,* T. Nakano,† S. Hirata,*
O. Kamigaito, M. Iwaki,‡ H. M. Shimizu, H. Kaneko, F. Hiei,§ Y. Sakemi, and S. Kobayashi
Department of Physics, Kyoto University, Kyoto 606, Japan

M. Yosoi** and H. Ikegami
Research Center for Nuclear Physics, Osaka University, Ibaraki, Osaka 567, Japan
(Received 10 June 1991)

We have measured the in-plane polarization transfer coefficients for the ^{6}Li(p,p') reaction using a longitudinally polarized beam at 65 MeV. A microscopic distorted-wave Born-approximation analysis with the M3Y interaction has been performed for the excitation to the first 0^+ state ($T=1$). The isovector tensor force $V_{T\tau}$ and the isovector spin-orbit force $V_{LS\tau}$ have been adjusted in order to reproduce the experimental differential cross sections, depolarization parameters, and in-plane polarization transfer coefficients. This analysis suggests that the high-momentum components of $V_{T\tau}$ should be substantially reduced from the M3Y interaction and $V_{LS\tau}$ needs to be more attractive.

PACS number(s): 25.40.Ep, 24.70.+s

Many experiments on the unnatural parity transition by proton inelastic scattering have been performed to study spin excitations, since the unnatural parity transition involves only $\Delta S=1$ amplitudes. Particularly, the isovector unnatural parity transition by proton inelastic scattering is useful in order to investigate the spin-dependent parts of the effective NN interaction because isovector unnatural parity states are well studied by electromagnetic transitions and those of $1p$- or $2s1d$-shell nuclei are well described by available shell-model wave functions. The effective interactions that are usually employed in the distorted-wave Born-approximation (DWBA) and distorted-wave impulse-approximation (DWIA) analyses are the local nucleon-nucleon (NN) t matrix or G matrix [1–4]. They can be written as

$$V=V_0+V_\tau\boldsymbol{\tau}_1\cdot\boldsymbol{\tau}_2+V_\sigma\boldsymbol{\sigma}_1\cdot\boldsymbol{\sigma}_2+V_{\sigma\tau}\boldsymbol{\sigma}_1\cdot\boldsymbol{\sigma}_2\boldsymbol{\tau}_1\cdot\boldsymbol{\tau}_2 + V_{LS}\mathbf{L}\cdot\mathbf{S}+V_{LS\tau}\mathbf{L}\cdot\mathbf{S}\boldsymbol{\tau}_1\cdot\boldsymbol{\tau}_2+V_TS_{12}+V_{T\tau}S_{12}\boldsymbol{\tau}_1\cdot\boldsymbol{\tau}_2 , \quad (1)$$

where S_{12} is a tensor operator. ^{6}Li is a $1p$-shell nucleus having a low-lying isovector unnatural parity state (0^+, $T=1$, $E_x=3.56$ MeV), which is well studied. Since this state is well separated, about 800 keV, from the nearest state, high-energy resolution is not needed. There have been several studies of the ^{6}Li(p,p') reaction for the transition to the first 0^+ state ($T=1$) under 100 MeV. Petrovich *et al.* analyzed the differential cross-section data near 45 MeV by the DWBA and reported that the $V_{\sigma\tau}$ part of the M3Y interaction [4] is about 40% too large [5]. Tosaki *et al.* measured differential cross sections $\sigma(\theta)$ and analyzing powers A_y at 65 and 80 MeV and also reported that the $V_{\sigma\tau}$ part of the M3Y interaction is too large [6]. As for the measurement of polarization transfer coefficients, Cornelius, Moss, and Yamaya measured depolarization parameters $K_y^{y'}$ at 32 MeV and compared their experimental data with the DWBA calculation using the Reid potential [7]. Sakai *et al.* measured $K_y^{y'}$ at 50, 65, and 80 MeV [8]. They did not discuss the effective interaction in that paper, but did report that the high-momentum components of $V_{T\tau}$ needs to be reduced to fit the ^{12}C(p,n)^{12}N reaction [9].

As noted above, many kinds of observable have been measured under 100 MeV, but polarization transfer coefficients have rarely been measured at the same incident energy in the same angular region where other observables have been studied. Moreover, no information on the in-plane polarization transfer coefficients $K_x^{z'}$ and $K_z^{x'}$ has been obtained. They are expected to be useful for investigating the spin-orbit force since they are sensitive to interference terms among the spin-orbit NN amplitude and the other NN amplitudes. We have measured the in-plane polarization transfer coefficients at 65 MeV and adjusted an available interaction so as to reproduce the measured observables.

We have measured the in-plane polarization transfer coefficients for excitation of the first 0^+ state in the ^{6}Li(p,p') reaction at 65 MeV. The experiment was performed by the double-scattering method with the longitudinally polarized beam at the Research Center for Nuclear Physics, Osaka University. By using the superconducting solenoid magnet system and two bending magnets in the beam transport, the longitudinal polarized beam with some sideways polarization component but no vertical polarization component is available on the beam

*Present address: Research Center for Nuclear Physics, Osaka University, Ibaraki, Osaka 567, Japan.

†Present address: Department of Physics, University of Alberta, Edmonton, Alberta, Canada T6G2N5.

‡Present address: Medical School, Osaka University, Suita, Osaka 565, Japan.

§Present address: Research Center, Sony Corporation, Yokohama 270, Japan.

**Present address: Department of Physics, Kyoto University, Kyoto 606, Japan.

 ©1992 The American Physical Society

line [10]. The longitudinal and sideways polarization components are obtained as $p_L = p_0 \sin\eta$ and $p_S = p_0 \cos\eta$ for the initial polarization p_0, where η is 292° at 65 MeV. The direction of the beam polarization was reversed between the spin-up and -down modes in 0.5-sec intervals. The sideways polarization component p_s and vertical polarization component p_N were continuously monitored by a polarimeter located upstream of the target during the measurement. The typical beam polarization values p_0 of spin-up and -down modes were 0.82 and 0.80, respectively. The vertical polarization p_N was less than 0.01. The beam intensity was about 200 nA on target.

A 95.4% enriched ^{6}Li foil of thickness 83.8 mg/cm^2 was used as a target. The contaminations, which are ^{7}Li, ^{12}C, ^{16}O, and ^{1}H, did not affect the final results of our measurement (see Fig. 1).

The scattered protons from Li were focused dispersively on the first focal plane (FP1) of the polarization spectrograph DUMAS [11]. Each proton was tagged by its momentum with the multiwire drift chamber (MWDC) on FP1. The MWDC was used because high spatial resolution was needed in order to obtain clear separation between the 0^+ state and continuum background corresponding to the ^{6}Li breakup channel. The spatial resolution of the MWDC was better than 250 μm full width at half maximum (FWHM). The tagged protons were focused archomatically on the second focal point (FP2) of DUMAS, where the multicarbon foil polarimeter MUSASHI [12] was placed. The scattering angle and energy of each proton scattered from carbon analyzer targets were measured by the upward or downward detectors (labeled by U or D) of MUSASHI.

For protons that were elastically scattered by analyzer targets of MUSASHI and that hit the downward (or upward) detector in the spin-up (or -down) mode, the momentum spectra on FP1 have been reconstructed. We have estimated the peak sum of the 0^+ state and continuum background by peak fitting the momentum spectra, where the shape of the background has been assumed to be linear. A reconstructed momentum spectrum is shown in Fig. 1.

The sideways polarization component on FP2, $p_{x''}$, measured with MUSASHI, is written as

$$p_{x''} = \frac{1}{\langle A \rangle} \frac{a-1}{a+1} , \quad (2)$$

where

$$a = \sqrt{(N_{\uparrow D} N_{\downarrow U})/(N_{\downarrow D} N_{\uparrow U})} ,$$

and $\langle A \rangle$ is the effective analyzing power. The N_{im}'s are the counting yields for the peak of the 0^+ state, where the subscript i refers to spin-up mode ($\uparrow$) or spin-down mode ($\downarrow$) and m refers to hitting the upward counter (U) or hitting the downward counter (D). The ratio a is used in order to reduce systematic errors from the ambiguities of the solid angles and efficiencies of the detectors and the integrated charge.

The $K_z^{x''}$ is defined as

$$K_z^{x''}(L,R) = p_{x''} \left[\frac{2}{p_{0\uparrow} + p_{0\downarrow}} \right] ,$$

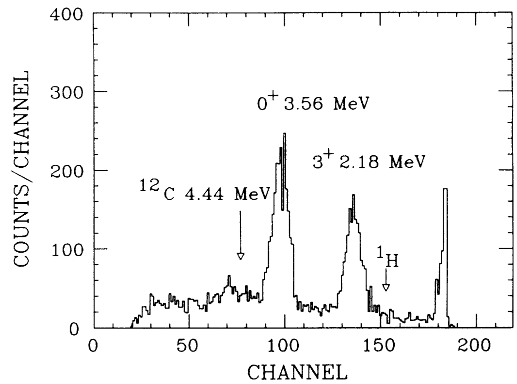

FIG. 1. Momentum spectrum reconstructed in spin-up mode for protons which are elastically scattered from analyzer targets of MUSASHI and hit down detector of MUSASHI. The first scattering angle is 10° on the left side of the beam direction. The arrows indicate the locations of possible peaks due to contaminants. There are no such peaks.

where $p_{0\uparrow}$ and $p_{0\downarrow}$ are the initial beam polarizations. The horizontal components of proton spin are rotated in the magnetic field of the DUMAS. Therefore, the $K_z^{x''}$ is a combination of $K_x^{x'}$, $K_z^{x'}$, $K_x^{z'}$, and $K_z^{z'}$, which are the usual in-plane polarization transfer coefficients in the laboratory frame:

$$K_z^{x''}(L,R) = (K_x^{x'} \cos\eta \pm K_z^{x'} \sin\eta) \cos\alpha \pm (K_x^{z'} \cos\eta \pm K_z^{z'} \sin\eta) \sin\alpha . \quad (3)$$

The precession angle of spin in the DUMAS, α, is calculated by

$$\alpha = \gamma \left[\frac{g}{2} - 1 \right] \theta_{\text{bend}} , \quad (4)$$

where $\theta_{\text{bend}} = 185°$ is the bending angle in the DUMAS, γ represents the Lorentz factor, and g is the Lande g factor. The L (R) and $+$ ($-$) signs correspond to the left (right) side measurement for the first scattering. As described in Eq. (3), the $K_z^{x''}(L)$ and $K_z^{x''}(R)$ at the same angle are independent observables. The first scattering angles were chosen to be 8° and 10° on both sides of the beam direction. The experimental data are shown in Fig. 2(a). The errors include counting statistics and the uncertainties in the data-reduction procedure.

The spin- and isospin-dependent terms of NN effective interactions, particularly tensor and spin-orbit forces, are examined by microscopic DWBA analysis (code DWBA74 [13] and modified by Nakai) of the excitation to the first 0^+ state because the $(LSJ;T) = (011;1)$ transfer is dominant in this excitation. In the DWBA analysis $K_z^{x''}(L,R)$ has been calculated by Eq. (3) in the laboratory frame and the other observables have been calculated in the center-of-mass frame. For the wave function of ^{6}Li, the $1p$-shell configuration of Cohen and Kurath [14] (CK wave function) has been chosen. The optical potential used is that of Ref. [6], which was obtained by fitting $\sigma(\theta)$ and A_y for p-^{6}Li elastic scattering at 65 MeV.

The M3Y interaction has been adjusted so as to reproduce the experimental $\sigma(\theta)$ [6] at forward angles, $K_y^{y'}$ [8] and $K_z^{x''}(L,R)$. $K_z^{x''}(L,R)$ is expected from PWIA to give information about the spin-orbit force since $K_x^{z'}$ and $K_z^{x'}$ in Eq. (3) include interference terms among spin-orbit NN amplitude and the other NN amplitudes. A_y is also expected to be sensitive to the spin-orbit force, but it is not used for the test of the NN interaction in this paper because A_y at forward angles is found to be more sensitive to the distorting potential than is the polarization transfer coefficient.

$\sigma(\theta)$ calculated using M3Y is about 2 times larger than the experimental data. As reported previously [5], good agreement is obtained for $\sigma(\theta)$ at forward angles when the spin-isospin-dependent central force $V_{\sigma\tau}$ is reduced. It is found that the central forces V_0, V_σ, V_τ, and $V_{\sigma\tau}$ affect $\sigma(\theta)$, but that their influence on $K_y^{y'}$ and $K_z^{x''}(L,R)$ at forward angles is small. On the other hand, tensor and spin-orbit forces have little effect on $\sigma(\theta)$ at forward angles. Therefore, tensor and spin-orbit forces can be investigated by analyzing $K_y^{y'}$ and $K_z^{x''}(L,R)$ without great care about the central forces. The reduced $V_{\sigma\tau}$ mentioned above is used in the adjustment of tensor and spin-orbit forces.

The short-range components of tensor and spin-orbit forces are thought to be ambiguous and mainly contribute through the (knock-on) exchange amplitude at forward angles. In this work only the short-range ($=0.25$ fm) components of the isovector tensor force $V_{T\tau}$ and isovector spin-orbit force $V_{LS\tau}$ are modified because it is impossible to distinguish between the isovector and isoscalar (contributing via only exchange amplitude) parts. The total χ^2 for $K_y^{y'}$ and $K_z^{x''}(L,R)$ is used as a guideline for the reproduction of the experimental values. The uncertainties of $K_z^{x''}(L,R)$ include not only statistical, but also systematic contributions from the data-reduction procedure, which are the same order as the statistical uncertainties. However, the χ^2 for $K_z^{x''}(L,R)$ has been calculated with only statistical uncertainty and for $K_y^{y'}$ by using the errors given in Ref. [8]. The results of the analysis are shown in Fig. 2. The minimum total χ^2 ($=9.26$) is obtained by adding an r^2 times Yukawa-type potential with strength of $-6000\pm600\,\mathrm{MeV\,fm^{-2}}$ and range of 0.25 fm to $V_{T\tau}$ and adding a Yukawa-type potential with strength of -2332 ± 990 MeV and range of 0.25 fm to the $V_{LS\tau}$ in the M3Y interaction. The uncertainties in the strengths are determined by the values where the total χ^2 increases 10% from the minimum one. Our analysis shows little correlation between $V_{T\tau}$ and $V_{LS\tau}$.

$V_{LS\tau}$ is limited by the analysis of both $K_z^{x''}(L,R)$ and $K_y^{y'}$. In contrast, $V_{T\tau}$ is strongly determined by only $K_y^{y'}$. This strong restriction on $V_{T\tau}$ by $K_y^{y'}$ enables $K_z^{x''}(L,R)$ to impose restrictions on $V_{LS\tau}$. In fact, because $K_z^{x''}(L,R)$ is sensitive to both $V_{T\tau}$ and $V_{LS\tau}$, it is necessary to fix $V_{T\tau}$ in order to investigate $V_{LS\tau}$ by fitting $K_z^{x''}(L,R)$. When $V_{T\tau}$ is fixed, $K_x^{z'}$ and $K_z^{x'}$ in the formula of $K_z^{x''}(L,R)$ are 10 times as sensitive to $V_{LS\tau}$ as $K_y^{y'}$ in the region $\theta_{\mathrm{lab}} \leq 15°$.

According to Ref. [1], $V_{T\tau}$ and $V_{LS\tau}$ around momentum transfer $k_A=1.5$ fm^{-1} contribute through the exchange amplitude in this energy region, where k_A is the momentum of incident nucleon in a nucleon-nucleus c.m. system, and they are substantially reduced in our modification (Fig. 3). This modification makes the total spin-orbit t matrix (including exchange) more attractive by about $10\,\mathrm{MeV\,fm^3}$ for the odd part and by about 4 MeV fm^3 for the even part in our angular region, as calculated by Eqs. (16) (replacing Q by k_A) and Eqs. (20) in Ref. [1]. They correspond to 30% (odd part) and 50% (even part) of the spin-orbit t matrix for M3Y. The total tensor t matrix includes the tensor operator, as Eq. (14) in

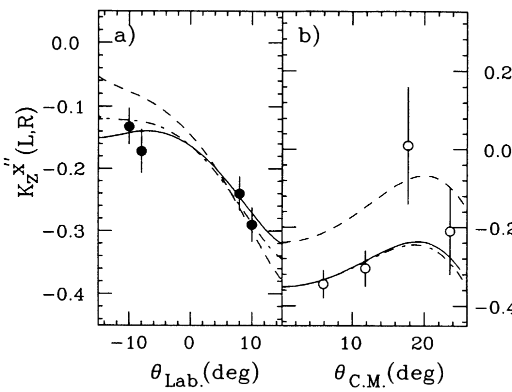

FIG. 2. Experimental data and the result of DWBA calculation for the in-plane polarization coefficient $K_z^{x''}(L,R)$ (this experiment, solid circle) and the depolarization parameter $K_y^{y'}$ (Ref. [8], open circle) are displayed in parts (a) and (b), respectively. The uncertainties of $K_z^{x''}(L,R)$ include not only statistical, but also systematic contributions from the data-reduction procedure, which are of the same order as the statistical. The dashed curve is M3Y, the dot-dashed curve represents M3Y with $V_{T\tau}$ modified, and the solid curve represents M3Y with $V_{T\tau}$ and $V_{LS\tau}$ modified (see text). In part (a) the + (−) sign of the scattering angle corresponds to the measurement on the left (right) side of the beam direction.

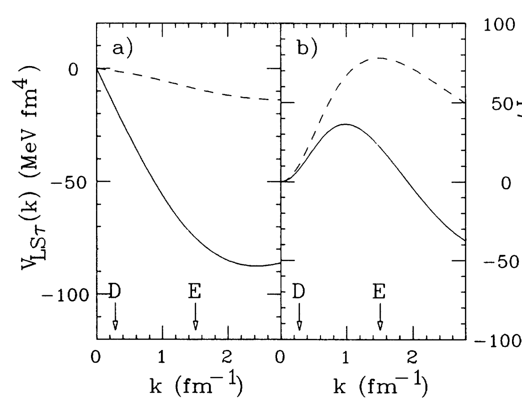

FIG. 3. Fourier transforms of $V_{LS\tau}$ and $V_{T\tau}$, the same as Eqs. (15b) and (15c) in Ref. [1], are shown in parts (a) and (b). The dashed curve is the M3Y. The solid curve is our modified M3Y ($V_{LS\tau}$ and $V_{T\tau}$ are modified). The momentum component around $1.5\,\mathrm{fm^{-1}}$ contributes through the exchange amplitude (arrow E) and that around $0.3\,\mathrm{fm^{-1}}$ contributes through the direct amplitudes (arrow D) in our measurement.

Ref. [1], and is not written as a simple function of momentum transfer. But our modification of $V_{T\tau}$ makes little change of the direct tensor term, and the contributions of our modification to the exchange tensor term are dominant. They are about 55 MeV fm^3 for the odd part and about 165 MeV fm^3 for the even part and, respectively, equivalent to 80% and 70% of the magnitudes of the exchange tensor t matrix for M3Y. Since $K_z^{x''}(L,R)$ contains the interference term between spin-orbit NN and central NN amplitudes, it is more sensitive to the change of spin-orbit force than $K_y^{y'}$. Thus high-accuracy measurement of $K_x^{z'}$ and $K_z^{x'}$ in a reaction with $(LSJ;T)=(011;1)$ transfer at forward angles is a useful tool for investigating $V_{LS\tau}$ of the effective NN interaction when other observables have been previously measured.

The experimental $K_y^{y'}$ at 50 and 80 MeV [8] are also reproduced much better by using this modified M3Y than by using M3Y. We have also performed the calculation using the density-dependent NN interaction of von Geramb at 100 MeV [3]. It is found that the experimental $K_y^{y'}$ at 65 and 80 MeV and $K_z^{x''}(L,R)$ at 65 MeV are also reproduced better by reducing its real $V_{T\tau}$ part around 1.5 fm^{-1}. Thus the high-momentum components of $V_{T\tau}$ seem to be less repulsive than in the effective NN interactions usually used. This reduction of the high-momentum components of $V_{T\tau}$ shows the same tendency as the effect of the ρ-meson coupling enhancement on the NN tensor potential [15,16]. Our modification for $V_{LS\tau}$ makes it more attractive than in M3Y, an effect similar to the influence of the ρ-meson coupling enhancement on the NN spin-orbit potential.

We have also used the following wave functions in order to check their influence on our results: (a) $1p$-shell LS coupling configuration [5]; (b) $1p, 1d, 2s$-shell configuration [17]. Within our calculation the differences caused by using different wave functions are small at forward angles and do not change the discussion above. However, Glover *et al.* analyzed $\sigma(\theta)$ and A_y for 0^+ excitations in (p,p') and (e,e') reactions and reported that more realistic shell-model configurations outside the $1p$ shell are important for a complete description of this transition at backward angles [18], which are outside of our measured region.

In summary, we have measured the in-plane polarization transfer coefficients $K_z^{x''}(L,R)$ in the ^{6}Li(p,p') reaction with a longitudinally polarized beam at 65 MeV. A microscopic DWBA analysis using the M3Y interaction was performed for the excitation to the first 0^+ state. The interaction was adjusted so as to reproduce the experimental $\sigma(\theta)$ at forward angles, $K_y^{y'}$ and $K_z^{x''}(L,R)$. When an r^2 times Yukawa-type potential with strength of -6000 MeV fm^{-2} and range of 0.25 fm is added to $V_{T\tau}$ and a Yukawa-type potential with strength of -2332 MeV and range of 0.25 fm is added to $V_{LS\tau}$ in the M3Y interaction, the experimental $K_y^{y'}$ and $K_z^{x''}(L,R)$ are excellently reproduced. Especially, the $K_z^{x''}(L,R)$ imposes restriction on the $V_{LS\tau}$. High-accuracy measurements of the in-plane polarization transfer coefficients $K_x^{z'}$ and $K_z^{x'}$ in a reaction with $(LSJ;T)=(011;1)$ transfer are useful for testing the $V_{LS\tau}$ part of the effective NN interaction.

Our modified M3Y also reproduces the experimental $K_y^{y'}$ at 50 and 80 MeV very well. When another effective NN interaction is used, its real part of $V_{T\tau}$ had better also be reduced in order to reproduce the experimental data. This reduction of the high-momentum components of $V_{T\tau}$ is consistent with the effect of the ρ-meson coupling enhancement on the NN tensor potential.

We would like to express our thanks to the staff of the cyclotron at RCNP for their kind cooperation during the experiment. We are grateful to Dr. J. A. Carr for his detailed answers to our questions on the wave function. This experiment was performed at RCNP under Program No. 26A19 and was supported in part by a Grant-in-Aid for Scientific Research No. 60420007, the Ministry of Science, Culture and Education in Japan.

[1] W. G. Love and M. A. Franey, Phys. Rev. C **24**, 1073 (1981).
[2] M. A. Franey and W. G. Love, Phys. Rev. C **31**, 488 (1985).
[3] H. V. von Geramb, in *The Interaction Between Medium Energy Nucleons in Nuclei (Indiana Cyclotron Facility, Bloomington, Indiana),* Proceedings of the Workshop on the Interactions Between Medium Energy Nucleons in Nuclei, edited by H. O. Meyer, AIP Conf. Proc. No. 97 (AIP, New York, 1982), p. 44.
[4] G. Bertsch, J. Borysowicz, H. McManus, and W. G. Love, Nucl. Phys. **A284**, 399 (1977).
[5] F. Petrovich, R. H. Howell, C. H. Poppe, S. M. Austin, and G. M. Crawley, Nucl. Phys. **A383**, 355 (1982).
[6] M. Tosaki, M. Fujiwara, K. Hosono, T. Noro, H. Ito, T. Yamazaki, H. Ikegami, and M. Kamimura, RCNP annual report, 1985, p. 21.
[7] W. D. Cornelius, J. M. Moss, and T. Yamaya, Phys. Rev. C **23**, 1364 (1981).
[8] H. Sakai *et al.*, Nucl. Instrum. Methods A **257**, 279 (1987).
[9] H. Sakai, K. Hatanaka, N. Matsuoka, T. Saito, A. Shimizu, M. Ieiri, K. Imai, and T. Motobayashi, J. Phys. G **10**, L139 (1984).
[10] M. Yosoi *et al.*, RCNP annual report, 1987, p. 189.
[11] T. Noro *et al.*, J. Phys. Soc. Jpn. Suppl. **55**, 61 (1986).
[12] M. Ieiri *et al.*, Nucl. Instrum. Methods A **257**, 253 (1987).
[13] R. Schaeffer and J. Raynal, code DWBA74 (unpublished), modified to calculate $K_z^{x''}(L,R)$ and use the density-dependent interaction of von Geramb [3].
[14] S. Cohen and D. Kurath, Nucl. Phys. **A73**, 1 (1965).
[15] G. E. Brown and M. Rho, Phys. Lett. B **237**, 3 (1990).
[16] E. J. Stephenson, in *Proceedings of the 7th International Conference on Polarization Phenomena in Nuclear Physics, Paris, France,* edited by A. Boudard and Y. Terrien [J. Phys. (Paris) Colloq. **51**, Suppl. 22, C6-85 (1990)].
[17] D. J. Millener and D. Kurath, Nucl. Phys. **A255**, 315 (1975).
[18] C. W. Glover *et al.*, Phys. Rev. C **41**, 2487 (1990).